# Theoretical insights into the mechanism of spiral $Ca^{2+}$ wave initiation in *Xenopus* oocytes

GENEVIÈVE DUPONT
*Unité de Chronobiologie Théorique, Faculté des Sciences, Université Libre de Bruxelles, B-1050 Brussels, Belgium*

**Dupont, Geneviève.** Theoretical insights into the mechanism of spiral $Ca^{2+}$ wave initiation in *Xenopus* oocytes. *Am. J. Physiol.* 275 (*Cell Physiol.* 44): C317–C322, 1998.—Spiral waves of intracellular $Ca^{2+}$ have often been observed in *Xenopus* oocytes. Such waves can be accounted for by most realistic models for $Ca^{2+}$ oscillations taking diffusion of cytosolic $Ca^{2+}$ into account, but their initiation requires rather demanding and unphysiological initial conditions. Here, it is shown by means of numerical simulations that these spiral $Ca^{2+}$ waves naturally arise if the cytoplasm is assumed to be heterogeneous both at the level of the synthesis and metabolism of D-*myo*-inositol 1,4,5-trisphosphate [Ins(1,4,5)$P_3$] and at the level of the distribution of the Ins(1,4,5)$P_3$ receptors. In such conditions, a spiral can be initiated in the simulations after an increase in Ins(1,4,5)$P_3$ concentration, with the direction of rotation being determined by the position of the region of high receptor density with respect to the locus of Ins(1,4,5)$P_3$ production.

oscillations; inositol 1,4,5-trisphosphate; spatiotemporal pattern

OSCILLATIONS AND WAVES OF cytosolic $Ca^{2+}$ have been observed in a large variety of cell types after stimulation by an extracellular agonist (3, 23). These oscillations occur through the periodic exchange of $Ca^{2+}$ between the cytosol and the internal stores (the sarcoplasmic or endoplasmic reticulum). Release of $Ca^{2+}$ from these stores is triggered by inositol 1,4,5-trisphosphate [Ins(1,4,5)$P_3$] synthesized by phospholipase C (PLC) in response to external stimulation. The Ins(1,4,5)$P_3$ receptor [Ins(1,4,5)$P_3$R] behaves as a $Ca^{2+}$ channel. Moreoever, the release of $Ca^{2+}$ through this channel is activated by cytosolic $Ca^{2+}$ itself (4, 11). The period of oscillations and the velocity of $Ca^{2+}$ wave propagation greatly depend on the cell type. The shape of the waves can also vary; in particular, immature *Xenopus* oocytes expressing muscarinic acetylcholine receptor subtypes can display circular, planar, and spiral $Ca^{2+}$ waves (16).

Extensive experimental and theoretical work has been carried out to uncover the mechanisms underlying $Ca^{2+}$ oscillations (3, 7, 20–23). After experimental results, in most models the autocatalytic regulation called $Ca^{2+}$-induced $Ca^{2+}$ release (CICR), by which $Ca^{2+}$ activates its own release from internal stores through the Ins(1,4,5)$P_3$R, is at the core of the oscillatory mechanism, although a mechanism based on the cross-activation of Ins(1,4,5)$P_3$ synthesis by $Ca^{2+}$ is also plausible (18). CICR can also explain the spatial propagation of planar and circular fronts resembling those observed experimentally, when the diffusion of $Ca^{2+}$ inside the cell is considered. Moreover, numerous features about these waves, such as their shape, rate of propagation, or the effect of $Ca^{2+}$ buffers, can be accounted for by considering detailed properties of the intracellular $Ca^{2+}$ dynamics (5a, 9, 15). Numerical simulations have shown that these models can also reproduce spiral $Ca^{2+}$ waves. However, in the literature, these spirals have been initiated with a rather arbitrary choice of initial conditions, which are often both exacting and unrealistic from a physiological point of view (2, 12, 15, 19).

In a previous study based on numerical simulations (10), it has been shown that the initiation of the spiral $Ca^{2+}$ waves observed in cardiac cells after overloading the stores can be explained by the spatial heterogeneity created by the nucleus (17). Such an assumption does not hold in *Xenopus* oocytes. These cells are indeed much larger than myocytes (1 mm in diameter vs. 100 μm in length); a small obstacle like a nucleus, behaving as a barrier to the propagation of excitation, is thus not able to break concentric waves to create spirals. In the present study based on numerical simulations, we propose a simple way by which spiral $Ca^{2+}$ waves could be initiated in *Xenopus* oocytes.

## DESCRIPTION OF THE SYSTEM

The propagation of concentric $Ca^{2+}$ waves has been extensively simulated by considering the diffusion of cytosolic $Ca^{2+}$ in the various models initially developed to account for $Ca^{2+}$ oscillations in homogeneous conditions (2, 9, 12, 15). Among these models, the one based on a phenomenological description of CICR is particularly well adapted for the study of $Ca^{2+}$ waves, as it contains only two variables; a detailed description of this model, which is used in the present numerical study to simulate the $Ca^{2+}$ dynamics in *Xenopus* oocytes, can be found elsewhere (8, 9, 12).

Spiral $Ca^{2+}$ waves generally arise from the asymmetric breaking of concentric waves. In a cell as large as the *Xenopus* oocyte, the asymmetry could arise from the existence of a gradient in Ins(1,4,5)$P_3$ concentration due to a spatially restricted synthesis of the latter

messenger. The substrate of PLC for Ins(1,4,5)$P_3$ synthesis is indeed located in the plasma membrane (3); moreover, the Ins(1,4,5)$P_3$ 5-phosphatase, the main enzyme responsible for Ins(1,4,5)$P_3$ metabolism, is mainly present on the cell surface (6). Thus, in our two-dimensional system designed to represent a portion of a *Xenopus* oocyte, it has been assumed that Ins(1,4,5)$P_3$ synthesis and metabolism only occur in a small region (*region 1* on Fig. 1) that is arbitrarily chosen as a square having a side of 27.8 μm. In this region, the time evolution of Ins(1,4,5)$P_3$ concentration (A) is given by

$$\frac{\partial A}{\partial t} = v_p - \epsilon A + D_A\left(\frac{\partial^2 A}{\partial x^2} + \frac{\partial^2 A}{\partial y^2}\right) \qquad (1)$$

in which $v_p$ is the rate of Ins(1,4,5)$P_3$ synthesis and $\epsilon$ is the first-order constant denoting the rate of Ins(1,4,5)$P_3$ degradation. $D_A$ stands for the diffusion coefficient of Ins(1,4,5)$P_3$ in the cytosol, the value of which has been measured in *Xenopus* oocytes (1). The two spatial coordinates are denoted $x$ and $y$, and $t$ is time. In the rest of the system (i.e., everywhere except *region 1* in Fig. 1), Ins(1,4,5)$P_3$ is assumed only to diffuse, i.e., $v_p = \epsilon = 0$. The gradient in Ins(1,4,5)$P_3$ concentration is expected to create a gradient in excitability that will favor the occurrence of a spiral wave if the $Ca^{2+}$ front possesses a free extremity (i.e., if a circular front has been broken); that the system exhibits differences in refractory times depending on the locus considered will indeed prevent the broken wave from reforming a concentric wave as it expends in this large system.

The breakage of the Ins(1,4,5)$P_3$-induced $Ca^{2+}$ wave can be provoked by some heterogeneity in the cytoplasm. On the basis of the assumption that the $Ca^{2+}$-releasing mechanisms are heterogeneously distributed in the cytoplasm, *region 2* in Fig. 1 is supposed to possess a higher density of Ins(1,4,5)$P_3$ receptor; this region is a square with 40.7-μm sides. From a quantitative point of view, the distinctive feature of this area is that the maximal velocity of $Ca^{2+}$ release from the internal stores has a larger value than in the rest of the system. The rate of release ($V_3$) now takes the form

$$V_3 = \alpha V_{M3} \frac{Y^2}{K_R^2 + Y^2} \frac{Z^4}{K_A^4 + Z^4} \frac{A}{K_D + A} \qquad (2)$$

in which, as in previous studies (9, 10), $V_{M3}$ stands for the maximal rate of $Ca^{2+}$ release and $K_R$ and $K_A$ are the threshold constants for release and activation, respectively. $K_D$ is the half-saturation constant of the Ins(1,4,5)$P_3$ receptor, and $\alpha$ is an adimensional number that allows for a possible increase in the density of Ins(1,4,5)$P_3$R. $Y$ and $Z$ are the intraluminal and cytosolic $Ca^{2+}$ concentrations, respectively. In the system schematized in Fig. 1, $\alpha = 1$ everywhere except in *region 2*, in which $\alpha = 3$.

The full system explicitly considers the evolution of Ins(1,4,5)$P_3$ concentration and of both intravesicular and cytosolic $Ca^{2+}$ concentrations. Diffusion of intravesicular $Ca^{2+}$ is not taken into account. A computer program was developed to numerically integrate these coupled partial derivative equations, using a variable time step Gear integration method. The dimension of the Cartesian grid used to simulate $Ca^{2+}$ and Ins(1,4,5)$P_3$ diffusion is 0.926 μm. The Laplacian is discretized using the finite difference method. No flux boundary conditions are used. This system of 270 × 270 × 3 differential equations is solved on Silicon Graphics R10000 workstation.

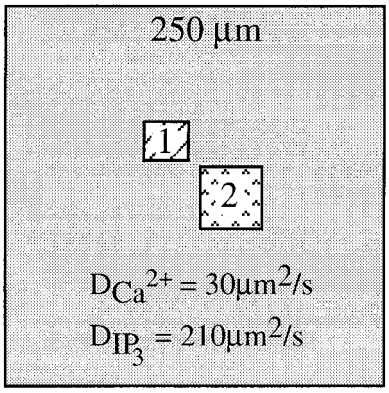


Fig. 1. Typical geometry of system used to study mechanism of spiral $Ca^{2+}$ wave initiation in *Xenopus* oocytes. Only 2 spatial dimensions are considered. Outer square represents a 250 × 250-μm portion of oocyte. Smaller inner square (*region 1*) is region in which D-*myo*-inositol 1,4,5-trisphosphate [Ins(1,4,5)$P_3$] synthesis and metabolism occur. Larger inner square (*region 2*) possesses a higher density of Ins(1,4,5)$P_3$ receptor than rest of system. For numerical integration, system is discretized in 270 × 270 grid points. In that frame, *region 1* has a side of 30 grid points and *region 2* has a side of 44 grid points. Top left corner of *region 1* is grid point with coordinates (100, 80); top left corner of *region 2* is grid point (137, 115). $D_{Ca^{2+}}$ and $D_{IP_3}$, diffusion coefficients for $Ca^{2+}$ and Ins(1,4,5)$P_3$, respectively, in cytosol.

## RESULTS

Numerical integration of the system defined in Ref. 10, in the geometry shown in Fig. 1, gives rise to spiral $Ca^{2+}$ waves. Such time-dependent, spatial structures of $Ca^{2+}$ are shown in Fig. 2; the three panels at *top* show the rather complex behavior that first arises when the rate of Ins(1,4,5)$P_3$ synthesis ($v_p$) is increased up to 8 $\mu M \cdot s^{-1}$. The $Ca^{2+}$ front is not circular because the regions close to the locus of Ins(1,4,5)$P_3$ synthesis are more excitable than the bulk of the system. After a transient period, the duration of which depends on the initial conditions, a more regular spiral $Ca^{2+}$ wave becomes visible and keeps on rotating clockwise. However, the spatiotemporal $Ca^{2+}$ pattern in the region possessing a higher density of Ins(1,4,5)$P_3$R (*region 2* in Fig. 1), which contains the tip of the spiral, remains irregular. The average wavelength of the $Ca^{2+}$ spiral is on the order of 130 μm, and the rotation time is slightly larger than 2 s; thus the wavelength is in good agreement with experimental observations, whereas the period is too short by a factor of two (12).

The complexity of the $Ca^{2+}$ dynamics in the region with a higher density of Ins(1,4,5)$P_3$R is visible by examination of the evolution of the level of cytosolic $Ca^{2+}$ at a particular grid point of this region. Such a time series [grid point (180, 135)] is shown in Fig. 3*A*. This region acts as a high-frequency pacemaker be-

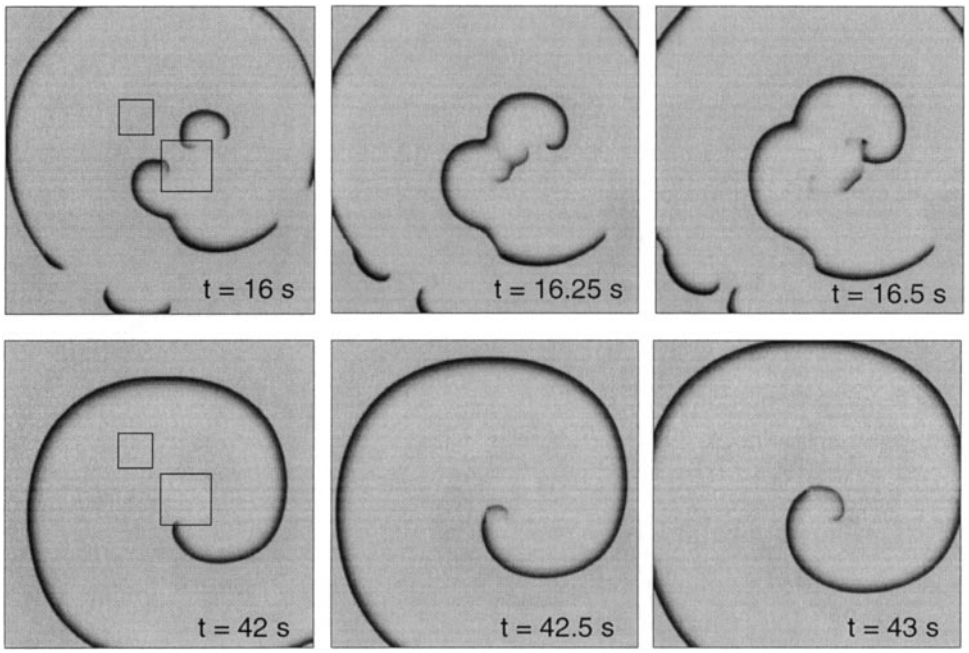


Fig. 2. Numerical simulation of a spiral $Ca^{2+}$ wave in a system that represents a portion of a *Xenopus* oocyte and has geometry shown in Fig. 1. Panels at *top* show how these waves first arise; panels at *bottom* represent the more regular spatiotemporal pattern, which is stable at least up to 300 s. Time ($t$) = 0 corresponds to time at which velocity of Ins(1,4,5)$P_3$ synthesis ($v_p$) in *region 1* (smaller square, see Fig. 1) increased from 0 to 8 $\mu M \cdot s^{-1}$. Initial conditions are at random for Ins(1,4,5)$P_3$ and $Ca^{2+}$. Color scale is linear between 0 (white) and 1.5 μM (black). Results were obtained by numerical integration of system defined in Ref. 10, with *Eqs. 1* and *2*, and with following parameter values: sum of basal and stimulated influx of $Ca^{2+}$ from extracellular medium ($V_{in}$) = 2.7 $\mu M \cdot s^{-1}$, maximal rate of $Ca^{2+}$ pumping into endoplasmic reticulum (ER) ($V_{M2}$) = 65 $\mu M \cdot s^{-1}$, threshold constant for $Ca^{2+}$ pumping ($K_2$) = 1 μM, maximal rate of $Ca^{2+}$ release from ER ($V_{M3}$) = 600 $\mu M \cdot s^{-1}$, threshold constant of release from ER ($K_R$) = 2 μM, threshold constant of activation ($K_A$) = 0.88 μM, passive flux of $Ca^{2+}$ from cytosol to external medium ($k$) and from ER to cytosol ($k_f$) = 10 and 1 $s^{-1}$, half-saturation constant of Ins(1,4,5)$P_3$ ($K_D$) = 1 μM, and $n$ = $m$ = 2 and $p$ = 4, where $n$, $m$, and $p$ are Hill coefficients for $Ca^{2+}$ pumping, release, and activation of release, respectively. In *region 1* (see Fig. 1) $v_p$ = 8 $\mu M \cdot s^{-1}$ and the first-order constant denoting rate of Ins(1,4,5)$P_3$ degradation ($\epsilon$) = 1 $\mu M \cdot s^{-1}$, whereas both quantities are 0 everywhere else. In *region 2* (larger square, see Fig. 1) the adimensional number that allows for a possible increase in density of Ins(1,4,5)$P_3$R ($\alpha$) = 3, whereas $\alpha$ = 1 everywhere else.

cause of the high rate of $Ca^{2+}$ release from the stores in this area. Only a fraction of the $Ca^{2+}$ spikes there initiated will be able to propagate in the surrounding region, which has a smaller potentiality to release $Ca^{2+}$. Thus the tip of the spiral sometimes breaks and finally disappears when it encounters a refractory region characterized by a basal density of Ins(1,4,5)$P_3$R. After some time, the new extremity of the front can bend again, thus forming a new tip. Alternatively, a new front is sometimes emitted by *region 2*, which is in the oscillatory regime; such a front then combines with the extremity of the large spiral, so that the global appearance of the $Ca^{2+}$ wave remains the same. The regular temporal evolution of cytosolic $Ca^{2+}$ in the grid point (120, 135), located in a region with a basal density of Ins(1,4,5)$P_3$R, is shown in Fig. 3*B*.

The respective locations of the regions of Ins(1,4,5)$P_3$ metabolism and synthesis, on the one hand, and of high Ins(1,4,5)$P_3$R density, on the other hand, play a crucial role in determining the occurrence of a spiral wave. In fact, to generate a spiral, the region of high receptor density has to be located in a steep gradient of Ins(1,4,5)$P_3$ concentration; as long as this condition is fulfilled, a phenomenon that depends on various counterbalancing factors such as the positions of the regions and the parameters $v_p$ and $\epsilon$, spiral waves do not accurately depend on the geometry of the system. For example, in a system like the one schematized in Fig. 1, the $Ca^{2+}$ wave still displays a spiral shape when *regions 1* and *2* are moved away from one another if, at the same time, $v_p$ is increased (not shown). Also, the shape and dimensions of these areas can be varied in the simulations without qualitatively affecting the spatiotemporal dynamics of cytosolic $Ca^{2+}$. In real cells, regions of high receptor density would certainly be distributed in a more random fashion. The effect of randomly distributed $Ca^{2+}$-releasing sites has already been investigated in other theoretical studies (5a, 15a). In such conditions, the waves can become abortive at small doses of Ins(1,4,5)$P_3$ or at very low density of Ins(1,4,5)$P_3$R; also, the front is more irregular, reflecting the inhomogeneous distribution of releasing sites. However, these studies clearly show that the continuous approximation certainly remains a good approximation of the qualitative behavior of the wave. In this respect, it appears that the occurence of spiral $Ca^{2+}$ waves would be little affected by a distribution of Ins(1,4,5)$P_3$R that is less regular than in the present

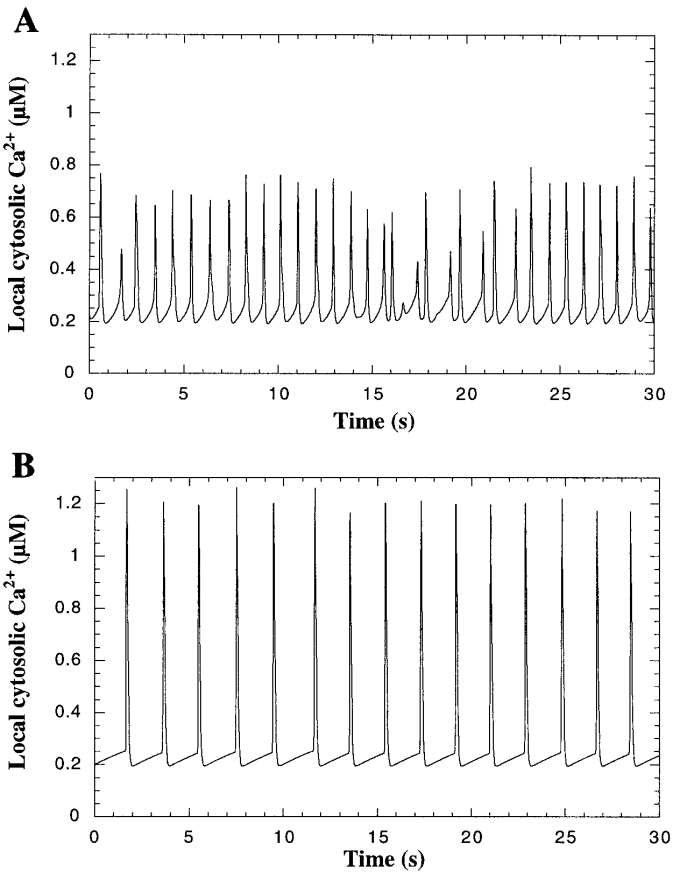


Fig. 3. Temporal evolution of local $Ca^{2+}$ concentration in a grid point, whose coordinates are (180, 135), located in region of high Ins(1,4,5)$P_3$R density (*A*) and of a grid point, with coordinates (120, 135), in bulk of system (*B*). $Ca^{2+}$ dynamics are much more complex in region of high receptor density, which acts as a high-frequency pacemaker surrounded by an excitable system. Equations, parameters, and configuration are same as in Fig. 2.

simulated system; the region that, on average, possesses a sufficiently higher density of Ins(1,4,5)$P_3$R would behave as the pacemaker site.

In experiments, $Ca^{2+}$ waves are often initiated by the injection or the photorelease of a poorly metabolizable analog of Ins(1,4,5)$P_3$ into the oocyte (16, 20). Such a situation can be simulated by considering that the level of Ins(1,4,5)$P_3$ is initially high in a well-defined region of the system that would correspond, for example, to the part of the oocyte that has been flashed. Moreover, it is then considered that this Ins(1,4,5)$P_3$ is not metabolized or synthesized ($v_p = \epsilon = 0$); the initially localized high level of Ins(1,4,5)$P_3$ spreads because of diffusion. This system, which also generates a gradient of Ins(1,4,5)$P_3$ concentration onto a region possessing a higher density of Ins(1,4,5)$P_3$R, can also generate spiral $Ca^{2+}$ waves. This is illustrated in Fig. 4, in which the larger, more central square (indicated for both $t = 9$ and $t = 10.25$) indicates the region of higher density of Ins(1,4,5)$P_3$R (same location as *region 2* in Fig. 1) and the other, smaller square shows the portion of the oocyte in which the level of Ins(1,4,5)$P_3$ was initially (i.e., at $t = 0$) at a higher level. As can be seen in the frame showing the situation at $t = 10.75$ s, the dynamics in the region of higher receptor density is complex, as in Figs. 2 and 3. In this particular case, the small "semicircular" front will not propagate further away outside the block because the surrounding medium is refractory. However, it will annihilate the part of the front that forms the tip of the larger spiral (see Fig. 4, $t = 11.75$)

An interesting change in the $Ca^{2+}$ spiral shown in Fig. 4 with respect to the one shown in Fig. 2 is that the former one rotates counterclockwise. This is due to the fact that the Ins(1,4,5)$P_3$ is now diffusing from the right side of the obstacle, whereas in Fig. 2 it was diffusing from the left side. This result does not depend on how the gradient in Ins(1,4,5)$P_3$ is generated [by a localized

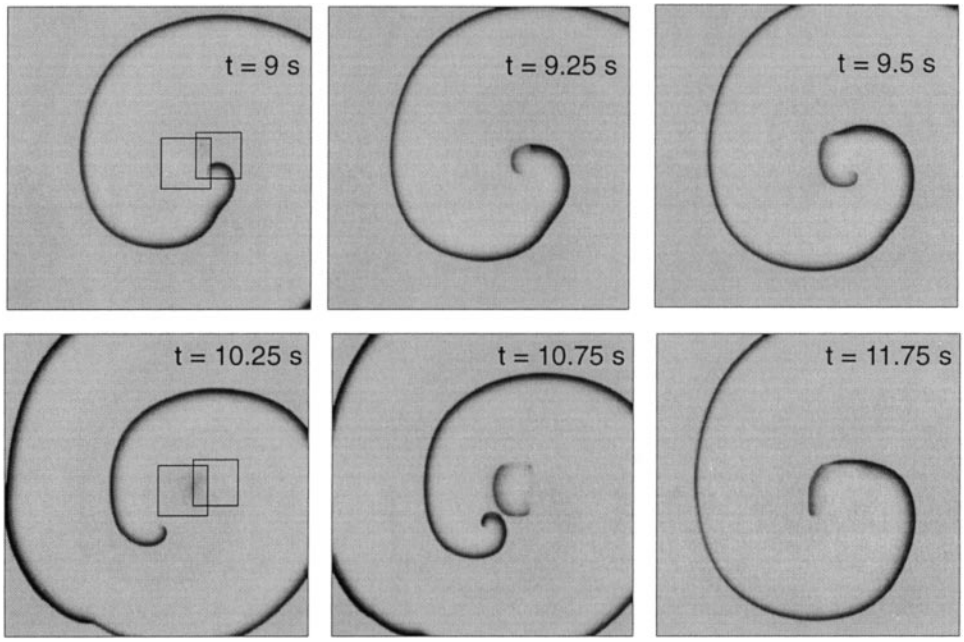


Fig. 4. Numerical simulation of a spiral $Ca^{2+}$ wave initiated by injection or photorelease of a poorly metabolizable analog of Ins(1,4,5)$P_3$. Counterclockwise rotation of spiral wave is due to fact that Ins(1,4,5)$P_3$ is diffusing from right side of block of higher receptor density, whereas in Fig. 2 it was diffusing from left side. At *left*, locations of these 2 regions are indicated [more central and larger square: higher density of Ins(1,4,5)$P_3$R; smaller square: region in which level of Ins(1,4,5)$P_3$ is initially (at $t = 0$) assumed to be at a high level of 22 μM]. Equations and parameters are same as in Fig. 2.

region of Ins(1,4,5)$P_3$ synthesis and metabolism or by an initially localized increase in Ins(1,4,5)$P_3$]. Such a counterclockwise rotation of the spiral can also be observed in the simulations in the same conditions as in Fig. 2, if the two areas indicated in Fig. 1 are moved in such a manner that *region 1* becomes located to the right of *region 2*. Although rather intuitive from a geometrical point of view (Figs. 2 and 4 are more or less mirror images), these differences make some physiological sense because the oocyte is polarized. Moreover, this prediction could be tested experimentally by injecting boluses of Ins(1,4,5)$P_3$ at various regions of the cell; the change of location of the pipette should in some cases induces a change in the direction of spinning of the spiral. Also interesting to mention is the fact that in Fig. 4, as in many other simulations, the spiral is only transient. Depending on the system, spirals rotating from 5 to ~25 times before their transformation into concentric waves have been observed in the simulations. Such transient $Ca^{2+}$ spirals have been reported experimentally (12). This contrasts with the situation shown in Fig. 2, in which the spiral appears as a stable spatiotemporal pattern (the stability has been tested until $t = 300$ s).

## DISCUSSION

It is well known that a circular front that breaks in an asymmetric medium can initiate a spiral. The present simulations show that this concept might explain the origin of the spiral $Ca^{2+}$ waves that have been observed in *Xenopus* oocytes. A region characterized by a higher density of Ins(1,4,5)$P_3$R can act as a source of heterogeneity that breaks the $Ca^{2+}$ wave, and the Ins(1,4,5)$P_3$ gradient due to either spatially restricted Ins(1,4,5)$P_3$ synthesis and metabolism or to injection of Ins(1,4,5)$P_3$ into a localized region of the oocyte can induce asymmetry of the medium. Moreover, this mechanism of spiral $Ca^{2+}$ wave initiation is rather robust with respect to changes in the values of the dynamic parameters or in the detailed configuration of the system that represents a portion of the cell. In that respect, it is reasonable to assume that a three-dimensional configuration corresponding to the spatial extension of the system schematized in Fig. 1 could generate scroll waves such as the ones occurring in oocytes.

In contrast with a previous study aimed at investigating the origin of spiral $Ca^{2+}$ waves in cardiac myocytes and in which an unexcitable region is responsible for spiral wave initiation, in the present work, spiral $Ca^{2+}$ waves are best initiated when the existence of a region possessing a larger potentiality to release $Ca^{2+}$ is assumed. If, in contrast, *region 2* (see Fig. 1) is assumed to have a lower density of Ins(1,4,5)$P_3$ than the rest of the system, a single $Ca^{2+}$ front is initiated in *region 1*, which is initially characterized by a high level of Ins(1,4,5)$P_3$; when it encounters the refractory region, the front breaks and propagates on both sides of the obstacle, after which, in most cases, both parts of the wave merge again into a circular front. Other numerical studies have shown that concentric $Ca^{2+}$ waves can sometimes transform into spiral ones when encountering refractory blocks; however, this mechanism is much less likely to occur in real cells, as some very precise relationships between the respective locations of the refractory block and the $Ca^{2+}$ front must be fulfilled.

That the microscopic spatial arrangement of the diverse processes involved in the $Ca^{2+}$ dynamics play an important role in determining the global aspect of the $Ca^{2+}$ waves has already been emphasized for various phenomena. For example, it has been shown that the saltatory nature of the $Ca^{2+}$ waves seen in HeLa cells (5) might be due to the inhomogeneous distribution of the Ins(1,4,5)$P_3$R throughout the cytoplasm (5a, 15a). In hepatocytes, it has been proposed that the $Ca^{2+}$ waves always originate from a specific locus, which differs from one cell to the other, because this region possesses a larger density of Ins(1,4,5)$P_3$R (24). Accordingly, in the present simulations, the block of higher receptor density acts as the initiation site for the $Ca^{2+}$ waves. In our system, this region (*region 2* in Fig. 1) is the only one to be in the oscillatory regime, as the rest of the cytoplasm is in an excitable state; such a difference is obtained by varying the local maximal velocity of $Ca^{2+}$ release ($\alpha V_{M3}$ in *Eq. 2*). In *Xenopus* oocytes themselves, the so-called "$Ca^{2+}$ puffs" are thought to originate from the opening of multiple Ins(1,4,5)$P_3$R gathered in clusters (20). Also, a gradient in the level of Ins(1,4,5)$P_3$ through the cell might explain the initiation point of the repetitive propagating fronts (13) and could play a role in the existence of kinematic $Ca^{2+}$ waves (14). Thus the spiral $Ca^{2+}$ waves that are frequently seen at the level of the entire *Xenopus* oocyte might simply result from the microscopic organization of the $Ca^{2+}$-releasing machinery.

## NOTE ADDED IN PROOF

Another plausible mechanism for spiral $Ca^{2+}$ wave initiation has been recently proposed by A. McKenzie and J. Sneyd (*Int. J. Bifurc. Chaos*. In press). In this study, spiral waves are initiated by simulating the release of Ins(1,4,5)$P_3$ at three different loci of the oocyte, in the absence of heterogeneity in the distribution of $Ca^{2+}$ stores.

I thank J. Lauzeral and J. Halloy for very fruitful discussions and A. Goldbeter for continuous support.

This work was supported by the "Actions de Recherche Concertée" Program (ARC 94-99) launched by the Division of Scientific Research, Ministry of Science and Education, French Community of Belgium.

G. Dupont is Chargé de Recherches at the Belgian Fonds National de la Recherche Scientifique.

Address for reprint requests: G. Dupont, Unité de Chronobiologie Théorique, Faculté des Sciences, Université Libre de Bruxelles CP231, B-1050 Brussels, Belgium.

Received 1 December 1997; accepted in final form 17 March 1998.

## REFERENCES

1. **Allbritton, N., T. Meyer, and L. Stryer.** Range of messenger action of calcium ion and inositol 1,4,5-trisphosphate. *Science* 258: 1812–1815, 1992.
2. **Atri, A., J. Amundson, D. Clapham, and J. Sneyd.** A single pool model for intracellular calcium oscillations and waves in the *Xenopus laevis* oocytes. *Biophys. J.* 65: 1727–1739, 1993.

3. **Berridge, M. J.** Inositol trisphosphate and calcium signalling. *Nature* 361: 315–325, 1993.
4. **Bezprozvanny, I., J. Watras, and B. Ehrlich.** Bell-shaped calcium response curves of Ins(1,4,5)$P_3$ and calcium-gated channels from endoplasmic reticulum of cerebellum. *Nature* 351: 751–754, 1991.
5. **Bootman, M., E. Niggli, M. Berridge, and P. Lipp.** Imaging the hierarchical nature of $Ca^{2+}$ signalling in HeLa cells. *J. Physiol. (Lond.)* 499: 307–314, 1997.

5a. **Bugrim, A., A. Zhabotinsky, and I. Epstein.** Calcium waves in a model with a random spatially discrete distribution of $Ca^{2+}$ release sites. *Biophys. J*. 73: 2897–2906, 1997.

6. **De Smedt, F., A. Boom, X. Pesesse, S. Schiffmann, and C. Erneux.** Post-translational modification of human brain type I inositol-1,4,5-trisphosphate 5-phosphatase by farnesylation. *J. Biol. Chem*. 271: 10419–10424, 1996.
7. **Dupont, G.** Spatio-temporal organization of cytosolic $Ca^{2+}$ signals: from experimental to theoretical aspects. *Comments Theor. Biol*. In press.
8. **Dupont, G., and A. Goldbeter.** One-pool model for $Ca^{2+}$ oscillations involving $Ca^{2+}$ and inositol 1,4,5-trisphosphate as co-agonists for $Ca^{2+}$ release. *Cell Calcium* 14: 311–322, 1993.
9. **Dupont, G., and A. Goldbeter.** Properties of intracellular $Ca^{2+}$ waves generated by a model based on $Ca^{2+}$-induced $Ca^{2+}$ release. *Biophys. J*. 67: 2191–2204, 1994.
10. **Dupont, G., J. Pontes, and A. Goldbeter.** Modeling spiral $Ca^{2+}$ waves in single cardiac cells: role of the spatial heterogeneity created by the nucleus. *Am. J. Physiol*. 271 (*Cell Physiol*. 40): C1390–C1399, 1996.
11. **Finch, E., T. Turner, and S. Goldin.** Calcium as a coagonist of inositol 1,4,5-trisphosphate-induced calcium release. *Science* 252: 443–446, 1991.
12. **Girard, S., A. Lückhoff, J. Lechleiter, J. Sneyd, and D. Clapham.** Two-dimensional model of calcium waves reproduces the patterns observed in *Xenopus* oocytes. *Biophys. J*. 61: 509–517, 1992.
13. **Jacob, R.** Calcium oscillations in endothelial cells. *Cell Calcium* 12: 127–134, 1991.
14. **Jafri, M., and J. Keizer.** Diffusion of inositol 1,4,5-trisphosphate, but not $Ca^{2+}$, is necessary for a class of inositol 1,4,5-trisphosphate-induced $Ca^{2+}$ waves. *Proc. Natl. Acad. Sci. USA* 91: 9485–9489, 1994.
15. **Jafri, M., and J. Keizer.** On the roles of $Ca^{2+}$ diffusion, $Ca^{2+}$ buffers, and the endoplasmic reticulum in $IP_3$-induced $Ca^{2+}$ waves. *Biophys. J*. 69: 2139–2153, 1995.

15a. **Keizer, J., and G. Smith.** Spark-to-wave transition: saltatory transmission of calcium waves in cardiac myocytes. *Biophys. Chem*. In press.

16. **Lechleiter, J., S. Girard, E. Peralta, and D. Clapham.** Spiral calcium wave propagation and annihilation in *Xenopus laevis* oocytes. *Science* 252: 123–126, 1991.
17. **Lipp, P., and E. Niggli.** Microscopic spiral waves reveal positive feedback in subcellular calcium signalling. *Biophys. J*. 65: 2272–2276, 1993.
18. **Meyer, T., and L. Stryer.** Calcium spiking. *Annu. Rev. Biophys. Biophys. Chem*. 20: 153–174, 1991.
19. **Othmer, H., and Y. Tang.** Oscillations and waves in a model of calcium dynamics. In: *Experimental and Theoretical Advances in Biological Pattern Formation*, edited by H. Othmer, J. Murray, and P. Maini. London: Plenum, 1993, p. 277–313.
20. **Parker, I., and I. Ivorra.** Confocal microfluorimetry of $Ca^{2+}$ signals evoked in *Xenopus* oocytes by photoreleased inositol trisphosphate. *J. Physiol. (Lond.)* 461: 133–165, 1993.
21. **Sneyd, J., J. Keizer, and M. Sanderson.** Mechanisms of calcium oscillations and waves: a quantitative analysis. *FASEB J*. 9: 1463–1472, 1995.
22. **Tang, Y., J. Stephenson, and H. Othmer.** Simplification and analysis of models of calcium dynamics based on $IP_3$-sensitive calcium channel kinetics. *Biophys. J*. 70: 246–263, 1996.
23. **Thomas, A., G. Bird, G. Hajnoczky, L. Robb-Gaspers, and J. Putney.** Spatial and temporal aspects of calcium signalling. *FASEB J*. 10: 1505–1517, 1996.
24. **Thomas, A., D. Renard, and T. Rooney.** Spatial and temporal organization of calcium signalling in hepatocytes. *Cell Calcium* 12: 111–127, 1991.